Experimental Investigation of the Effect of Speckle Noise on Continuous Scan Laser Doppler Vibrometer Measurements

Michael W. Sracic
&
Matthew S. Allen

University of Wisconsin-Madison
535 Engineering Research Building
1500 Engineering Drive
Madison, WI 53706

Abstract
Continuous Scan Laser Doppler Vibrometry (CSLDV) sweeps a laser spot continuously over a structure to measure its mode shapes at hundreds of points simultaneously. It can be used to measure accurate, detailed mode shapes using a hand-held impact hammer, while conventional point-by-point LDV can be impractical and inaccurate in that application because of strike-to-strike variation in the impact location and orientation. Recently presented techniques can be used to transform the CSLDV measurements into a set of responses that can be processed using standard system identification techniques to extract the modes. The resampling method works best when the scan frequency is high relative to the highest natural frequency of interest, and state of the art scanning vibrometers are capable of relatively high scan frequencies, but there is a tradeoff between measurement quality and scan frequency due to laser-speckle noise. This work explores the effect of LDV measurement noise, both the periodic and non-periodic components, on CSLDV measurements. Of particular interests are: the dependence of the signal-to-noise ratio on the scan rate and geometry, the target-to-detector distance of the experimental setup, the Doppler signal quality, and the sampling rate used to acquire the measurement. The results presented sometimes seem contrary to one's intuition and to the conclusions presented in other works, but they do provide a fairly thorough guide for the experimentalist, enabling the design of CSLDV experiments with the minimum noise level possible.

Nomenclature

t	:	Temporal Variable	N_o	:	# of Samples per Period
x	:	Spatial Variable	N_{aper}	:	# of Non-Periodic Signal Values
x_m	:	Maximum Spatial Value	$N_{aper,lifted}$	:	# of lifted Non-Periodic Values
λ	:	Wavelength Variable	T_A	:	Signal Period
φ_i	:	Phase Variable	v	:	Voltage Signal
f_{samp}	:	Sampling Frequency	y	:	Response Signal
f_{scan}	:	Scanning Frequency	y_n	:	nth Pseudo Response Signal
h	:	Surface Imperfection Height	y_{per}	:	Periodic Data of Response Signal
d	:	Target-to-Detector Distance	$Y_{aper}(\omega)$	:	Non-Periodic Frequency Signal
θ	:	Laser Sweep Angle	$Y_{aper,lifted}(\omega)$	:	Lifted Non-Periodic Freq. Signal
η_{ave}	:	Non-Periodic Noise Average	$\eta_{ave,lifted}$	:	Lifted Non-Periodic Noise Average
ρ_{ave}	:	Periodic Noise Average			

1. Introduction

Laser Doppler Vibrometry (LDV) has become increasingly common for vibration measurements because it provides a non-contact measurement with excellent bandwidth and allows one to measure the response of a surface at thousands of points using automated software. The conventional approach involves illuminating a

single point on an object, acquiring a measurement, and then using automated scanning mirrors to reposition the laser spot and repeat the process at numerous other points on the structure. This is clearly more convenient than the time consuming setup involved with other measurement devices such as force transducers and accelerometers, and is generally more accurate than roving hammer tests. However, if each measurement record is long, as is the case for a structure with low natural frequencies, the LDV still may require excessive time to collect a set of measurements. Furthermore, the measurements acquired using traditional LDV may be inconsistent if the structure has the potential to change with time, temperature or other factors. Stanbridge, Ewins and Martarelli [1] advanced a technique, which was originally presented by Sriram *et al.* [2-4], that overcomes some of these limitations by scanning the laser spot continuously over the surface of a test device while acquiring a measurement, allowing one to simultaneously acquire temporal information as well as spatial information at hundreds or thousands of points simultaneously. The shape of the scan pattern is dictated by computer-controlled mirrors, so virtually any shape can be used.

A few different techniques have been presented by which one can determine the mode shapes of a linear system from CSLDV measurements. Original efforts in continuous scan laser Doppler vibrometry (CSLDV) by Sriram *et al.* used broadband excitation and sampled synchronous with the laser scan speed to generate traditional Frequency Response Functions (FRFs) [2], although they seem to have abandoned that approach due to high noise levels. Stanbridge *et al.* presented a method whereby the structure is excited near resonance for a certain mode, and a Fourier analysis leads to a polynomial series description of the mode shape. They have also successfully identified multiple modes of a structure using impact excitation and CSLDV [5, 6], using an approach that is usually successful so long as the structure has lightly damped modes with relatively high natural frequencies. The authors recently presented a technique [7, 8] that allows one to extract the modes of a structure using conventional modal analysis routines, by decomposing the response into a set of responses that would have been measured at each point along the scan path if the laser spot were held stationary. The decomposition has been referred to as a “lifting” technique in the context of general time-periodic systems [9-12]. This technique also allows one to apply standard tools such as Mode Indicator Functions, to identify modes with close natural frequencies. Although outstanding correlation has been observed between the identified and analytical frequencies and mode shapes in a few preliminary applications, relatively little is known regarding the influence of noise and the potential thresholds for scanning rates and other experimental test parameters.

The occurrence of noise affects all applications of laser-type transducers. When coherent (laser) light is reflected off of an optically rough surface, granule-like imperfections on the device’s surface with size on the order of hundreds of nanometers act to dephase the light returning from the surface, causing bright and dark regions where the light constructively and destructively interferes. Relative motion between the laser spot and the surface causes the speckle pattern to evolve, producing a spurious vibration-like signal that cannot be easily distinguished from the true vibration.

Laser speckle has been investigated for decades in various contexts, although its influence on laser vibrometry has only been appreciated more recently. Previous works have noted the dependence of the speckle pattern on several key factors. The size of the incident light wave front greatly influences the appearance of a speckle population. Smaller diameter laser spots reflect more developed speckle patterns; individual speckles reflected from a smaller sized laser spots are larger in appearance and there are more regularized light and dark intensity patterns [13, 14]. The target surface and any motion it undergoes also affects laser speckle. A polished metallic surface produces a speckle pattern with an intensity envelope due to the polishing direction but the finer inconsistencies of the polished surface prevents structured speckle patterns within that envelope. Retro-reflective tape, which is a surface treatment that consists of micro-scale glass beads, causes reflected light to scatter in a concentrated cone surrounding the incident light direction, and produces well developed Airy-function type intensity patterns [13, 14]. In-plane translation and out-of-plane rotation of the test device have been found to significantly affect laser speckle patterns and the way they change. Rothberg and Halkon [15] have shown that pure rotation of the target surface out of the target plane perpendicular to the optical axis of a laser setup will tend to cause a translation of the laser speckle pattern with little or no speckle “evolution”. Alternatively, a pure translation of the target surface within the target plane will cause the reflected speckle pattern to “evolve” or “boil” as it has been termed in the past [16].

Rothberg [17] used Fourier optics to investigate the effects of a typical laser vibrometer setup on the speckle patterns produced in the scattered light. He theorized that the detected speckle signals would contain time dependent intensity and phase information for non-normal surface vibrations, and then observed effects of certain

target motions on the back scattered speckle patterns. For a laser vibrometer incident on a rotating shaft, Rothberg noted that frequency domain amplitude peaks occurred at the shaft's rotation frequency and harmonics and suggested that the speckle noise is approximately periodic. This has been attributed to the fact that the laser spot traces the same path on the surface, resulting in a periodically-varying speckle pattern. However, a perfectly periodic speckle pattern would require that the laser trace the exact same path over the rough surface, with consistency on the order of the light wavelength (100's or nanometers), during each period. Clearly this level of consistency cannot be expected due to vibration or motion of the test device, but those factors notwithstanding, speckle noise is observed to be predominantly periodic in most applications. Martarelli and Ewins [18] noted that speckle noise is also nearly periodic in CSLDV measurements, and compared the harmonic and non-harmonic components (sidebands) of the speckle noise between 0.2 and 20 Hz scanning frequencies. Their results show that noise level increases with increasing scan frequency, although the authors have successfully utilized scanning frequencies as high as 100 Hz, so there is a desire to extend that work to higher scan frequencies. Furthermore, the analysis method used by the authors is somewhat immune to the periodic component of the speckle noise, whereas that was the primary focus in [18].

For example, Figure 1 displays the composite FRFs, the data-fits achieved from using the AMI algorithm [10] and the difference between data and the fits of the lifted or time-invariant signals for a CSLDV measurement of the free response of an aluminum beam excited with an impact hammer. The measurement was acquired by scanning an LDV with a sinusoidal driving function at 100 Hz and the sampling frequency was 81.9 kHz, producing 820 pseudo-points per 100 Hz cycle. The bandwidth of the lifted signal f_{max}, is equal to half of the scanning frequency, so higher frequencies are effectively aliased into this bandwidth, as illustrated in [8]. After identifying the modes of the system, a noise floor remains (red curve) whose amplitude is comparable to that of some of the weakly excited modes. This work seeks to discover ways of designing the CSLDV experiment to minimize this noise level.

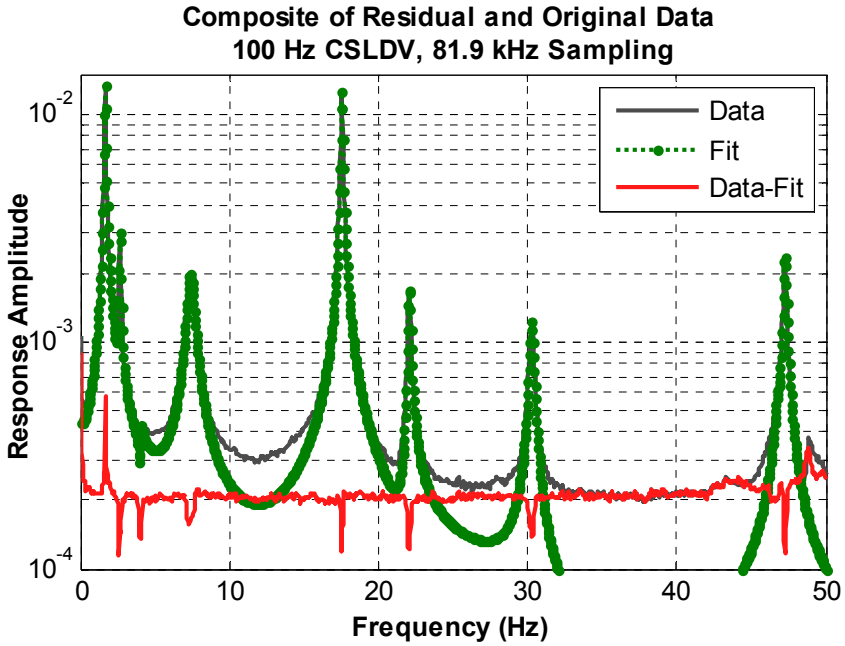

Figure 1: Composite FRFs of lifted CSLDV response with 100 Hz scanning frequency and curve fit obtained by modal parameter identification algorithm. The red curve shows a composite of the difference between the two, which is an indication of the noise level.

This paper presents the results of a number of experiments aimed at characterizing both the periodic and non-periodic laser speckle noise in CSLDV applications, and to determine how it is affected by the geometry of the test setup, the sampling rate, and other factors so that optimal parameters can be identified. The following section reviews some relevant theory regarding CSLDV and laser speckle. Section 3 presents the results of a series of experiments in which a number of parameters were varied to characterize how each affects the speckle noise. Conclusions are presented in Section 4.

2. Effects of Speckle Noise on CSLDV

2.1. CSLDV Theory

The signal measured from a LDV incident on a freely vibrating, linear, time-invariant structure can be represented by the summation of decaying exponentials made up of modal components as:

$$y(t) = \sum_{r=1}^{2N} \phi(x)_r \, C_r e^{\lambda_r t}$$
$$\lambda_r = -\zeta_r \omega_r + i\omega_r \sqrt{1-\zeta_r^{\,2}} \;\; , \;\; \lambda_{r+N} = -\zeta_r \omega_r - i\omega_r \sqrt{1-\zeta_r^{\,2}} \qquad (1)$$

where λ_r is the r^{th} eigenvalue, made up of the r^{th} natural frequency ω_r, and damping ratio ζ_r. The corresponding mode vector $\phi(x)_r$ depends on the position x of the laser beam along its path. This path could involve motion in three dimensions in a general case. C_r is the complex amplitude of mode r, which depends upon the structure's initial conditions, or on the impulse used to excite the structure if such an excitation is employed.

When using CSLDV, the laser is assumed to trace out a known periodic path of period T_A, such that $x(t) = x(t+T_A)$, or with the scan frequency $\omega_A = 2\pi/T_A$, resulting in a change from spatial to temporal dependence of the mode vector.

$$y(t) = \sum_{r=1}^{2N} \phi(t)_r \, C_r e^{\lambda_r t}$$
$$\phi\left(x(t)\right)_r = \phi(t)_r = \phi\left(t + T_A\right)_r \qquad (2)$$

This is identical to the expression for the free response of a Linear Time Periodic (LTP) system [19]. Two methods have been proposed to determine $\phi(t)_r$ and λ_r in eq. (2), the Fourier Series expansion method and the lifting method.

2.1.1. Fourier Series Expansion Method

If the CSLDV scan pattern is periodic, then mode shapes $\phi(t)_r$ can be expanded into a Fourier Series as follows,

$$\phi_r(t) = \sum_{m=-N_B}^{N_B} B_{r,m} \exp(im\omega_A t) \qquad (3)$$

where it is assumed that only the coefficients running from $-N_B$ to $+N_B$ are significant. Substituting into eq. (2) and moving the summations to the outside results in the following.

$$y(t) = \sum_{r=1}^{2N} \sum_{m=-N_B}^{N_B} B_{r,m} \exp\left(\left(\lambda_r + im\omega_A\right)(t - t_0)\right) \qquad (4)$$

This is mathematically equivalent to the impulse response of an LTI system with $2N(2N_B + 1)$ eigenvalues

$$\lambda_r + im\omega_A. \qquad (5)$$

Note that the amplitude of each harmonic $B_{r,m}$ in eq. (4) are the Fourier coefficients for the r^{th} mode and the m^{th} Fourier Term. It is important to characterize the frequency content of the laser speckle noise so that it can be discerned from the meaningful harmonics in the response, because both can appear as narrow-band spikes in the spectrum. Stanbridge, Martarelli and Ewins use a very similar approach, although they allow non-periodic scan patterns and identify a power series model for the operating shape.

2.1.2. Lifting Method

The lifting method eliminates the time dependence of $\phi(t)_r$ in eq. (2) by sampling the signal $y(t)$ from the LDV discretely such that the laser's position is $x(t_i) = x_i$ (corresponding to a specific point along the laser's path each period). A linear time-periodic signal, sampled as such, can be reorganized according to:

$$\begin{aligned} y_0 &= [y(0), y(T_A), y(2T_A), \cdots] \\ y_1 &= [y(\Delta t), y(\Delta t + T_A), y(\Delta t + 2T_A), \cdots] \\ y_2 &= [y(2\Delta t), y(2\Delta t + T_A), y2(\Delta t + 2T_A), \cdots] \\ &\cdots \\ y_{N_o-1} &= [y((N_o-1)\Delta t), y((N_o-1)\Delta t + T_A), y((N_o-1)\Delta t + 2T_A), \cdots] \end{aligned} \tag{6}$$

where N_o is the ratio of the sampling frequency to the periodic signal frequency, $N_o = f_{samp}/f_{scan}$. Each y_i in eq. (6) (called a pseudo-response point because it was extracted from the measured signal $y(t)$) now can be represented by a time-invariant system, and can be transformed into the frequency domain using the Discrete Fourier Transform (DFT) and processed with any standard identification routine. The results of utilizing the lifting technique to process free response CSLDV data is thoroughly presented in [7] and [8].

Because the lifting method reorganizes CSLDV data according to the period of the scanning frequency, the periodic component of the speckle noise is deposited on the zero frequency line in the lifted spectrum. Any sidebands to the periodic component are also deposited around this zero line as well.

2.1.3. Sampling Frequency

When testing with CSLDV, sampling faster provides more spatially dense information, which is beneficial for applications such as damage detection or providing detailed mode shapes. In terms of laser speckle, increased sampling has the effect of allowing the detector to see more speckle patterns per period each with a different and nominally "random" phase distribution. However, one also obtains a larger number of lifted responses, or pseudo-response points x_i as the sample rate increases, as is readily apparent from eq. (6). Hence, there is a tradeoff between identifying a larger number of points, which may serve to average out errors, and collecting more speckle noise as the sampling rate increases. The scenario is somewhat different for the Fourier Series expansion method, because the bandwidth of the CSLDV signal is determined by both the natural frequencies of the system and by the total number of Fourier terms required to represent each mode shape. The bandwidth needs to be large enough such that all of the Fourier terms that stand out above the noise floor are captured, and capturing additional bandwidth adds no significant information. Of course, meaningful mode shapes are not obtained unless a large enough number of Fourier terms stand out above the noise, so it important to take steps to minimize the nosie. One focus of this work will be to characterize the effect of the sample bandwidth on speckle noise..

2.2. Laser Speckle Theory

Nearly all engineering surfaces can be described as optically rough, which means that the imperfections in the surface are on the order of the wavelength of light. When coherent light is incident on such a surface, the variation of surface features disperses the incident rays causing them to reflect in nearly all directions. Neighboring "bumps" will de-phase adjacent rays, and complex interference patterns then arise giving "laser speckle" its name because of the appearance of speckling of bright and dark features within such a pattern. Figure 2 shows a representation of an incident wave front being de-phased upon reflection by an optically rough surface.

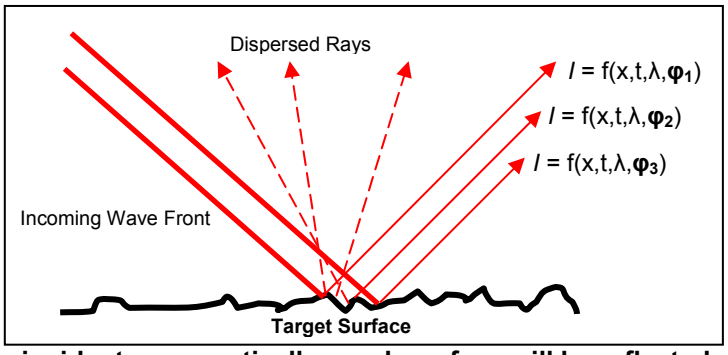

Figure 2: Wave fronts incident on an optically rough surface will be reflected and dispersed due to surface features. Adjacent reflected rays will contain different phase information and the intensity represented by the summation of rays on a detector will combine adjacent rays and phase information will cause light and dark interference patterns, or speckle.

2.2.1. Laser Spot Size and Shape

Martin and Rothberg [14] have shown the strong dependence of speckle size on laser spot diameter. In fact, they observed that for a variety of surfaces, a 600 μm laser spot diameter produces smaller sized speckles than a 100 μm laser spot diameter because the larger illuminated area reflects greater numbers of random phase distributed intensity regions leading to more destructive interference patterns

Most commercial scanning vibrometers have focusing features that in the standard operation mode refocus the laser spot each time it changes position. Refocusing is not practical when operating in continuous scanning mode, so the focus varies depending on the position of the spot within the target plane. The laser spot size is at its minimum diameter in the focal plane, becoming larger as the spot strays from this plane (See Figure 3). Note also from Figure 3 that the different spatial variables of the scan can be related by the following equation:

$$\tan\theta = \frac{x_m}{d} \tag{7}$$

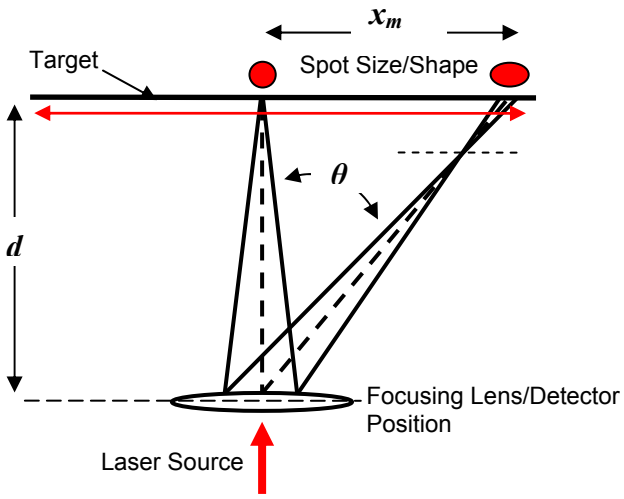

Figure 3: The size and shape of the laser spot change as it is scanned in one dimension.

One school of thought suggests that speckle noise should be at a minimum if the laser source is focused to its aperture limited focal size on the target because this produces only one (or a very small number) of large speckles that are about the same size as the detector being used. (Theoretical focal points have zero dimensions, but real optical systems are practically limited by one or more aperture sizes [20].) As motion is

introduced, this single speckle will transition out of the detector, but one would hope that the transition is mild because the speckle is large. According to this theory, as the laser spot increases in size one obtains a larger number of smaller speckles on the detector. In any instant many of these may transition off of the detector causing speckle noise.

Figures 4 and 5 illustrate this effect for an aluminum beam. The Polytec vibrometer described subsequently was focused on the beam's surface, and the field of laser light reflected from the surface to a target near the front of the LDV was recorded with a digital camera. When the laser beam is focused carefully on the beam's surface, a pattern with relatively large speckles is obtained at the detector, as shown in Figure 4. This presumably places about one speckle on the detector of the LDV. On the other hand, the spot size increases as laser beam is swept away from the best focus point, producing smaller sized speckles, such as those shown in Figure 5. The bright vertical band in the speckle pattern is probably due to extrusion lines on the surface of the beam. It has been suggested that one may reduce speckle noise for some kinds of surface motions by defocusing the laser beam [15], which would imply that one might observe either an increase or decrease in noise as the laser spot moves along the surface of a structure. This will be evaluated in Section 3.1.

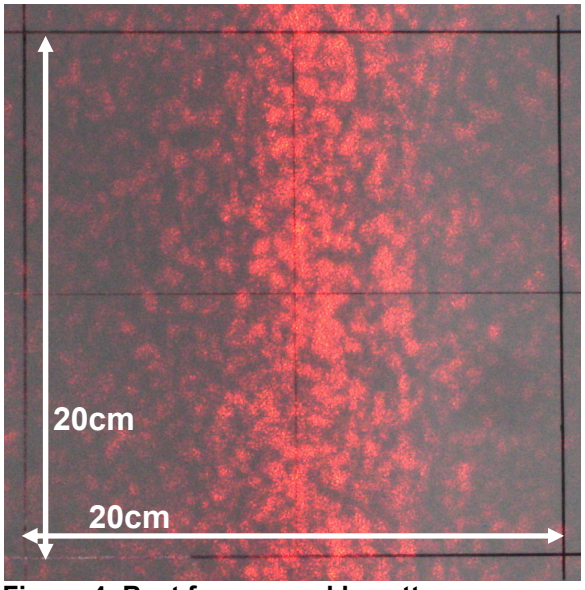

Figure 4: Best focus speckle pattern with smallest laser spot size.

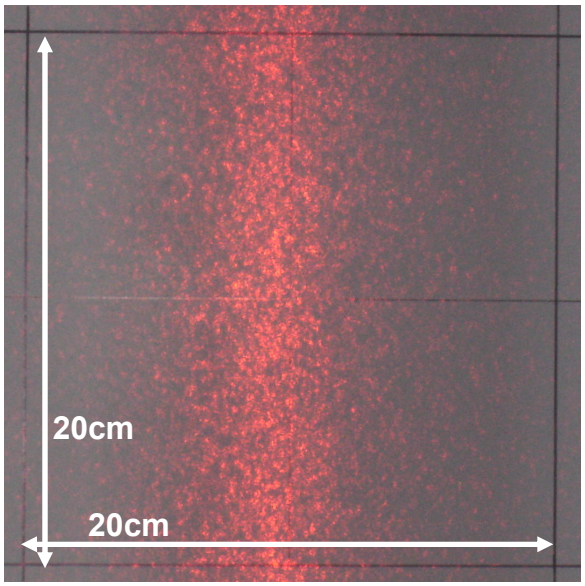

Figure 5: Speckle pattern with larger laser spot size due to being slightly out of focus.

3. Experimental Investigation of CSLDV Speckle Noise

In order to quantify the speckle noise present in CSLDV signals, measurements were acquired under nearly zero vibration conditions, but while scanning the laser spot sinusoidally at various frequencies. A Polytec® PSV-400 scanning laser vibrometer was employed, and the same aluminum beam used in [8] and [7] was used as the target. A number of parameters of the experimental setup were varied to assess the effect of each on the speckle noise, including: scan length, target-to-detector distance and sampling rate. The qualitative results of the speckle noise on the CSLDV process, in particular the effects of surface velocity, were noted. Quantitative measures of the average levels of both the periodic and non-periodic components of speckle noise were found for various combinations of the experimental parameters. The following tables provide the values of the experimental parameters used in the study with the nomenclature from Figure 3.

Scan Length	Target-to-Detector Separation	Sampling Frequency
$2*x_m$, [m]	d, [m]	$f_{samp,}$[kHz]
0.3	2	12.8
0.6	3.4	25.6
0.98	5.5	51.2

Table 1: Experimental parameters used in noise study.

Scan Frequency, f_{scan},[Hz]											
5	10	15	20	30	40	50	60	70	80	90	100

Table 2: Experimental scanning frequencies used in noise study.

The scan frequency was varied by 10 Hz from 20-100 Hz for scan lengths $2*x_m$= 0.3, 0.6, and 0.98 meters at each of target-to-detector separations d=2, 3.4 and 5.5 meters. At the closest target-to-detector separation tested, d=2 meters, scan frequencies of 5 Hz, 10 Hz, and 15 Hz were also investigated to overlap with other published studies. Since surface velocity has been shown to be influential to speckle noise, it was chosen to be the independent variable in most of the following plots.

3.1. Experimental Surface Velocity Noise Results

Figure 6 shows the frequency domain vibrometer signal from a sinusoidal continuous scan at a frequency of 10 Hz on a slender aluminum beam. Sharp peaks can be seen at integer multiples of 10 Hz for the entire bandwidth of the sampling space, the majority of which is not plotted. Based on previous work, one would attribute these peaks to periodic speckle noise. The noise away from these frequency lines is about one order of magnitude lower. Also, the magnitude of the first fundamental frequency and first few harmonics is nearly twice that of the rest of the harmonics.

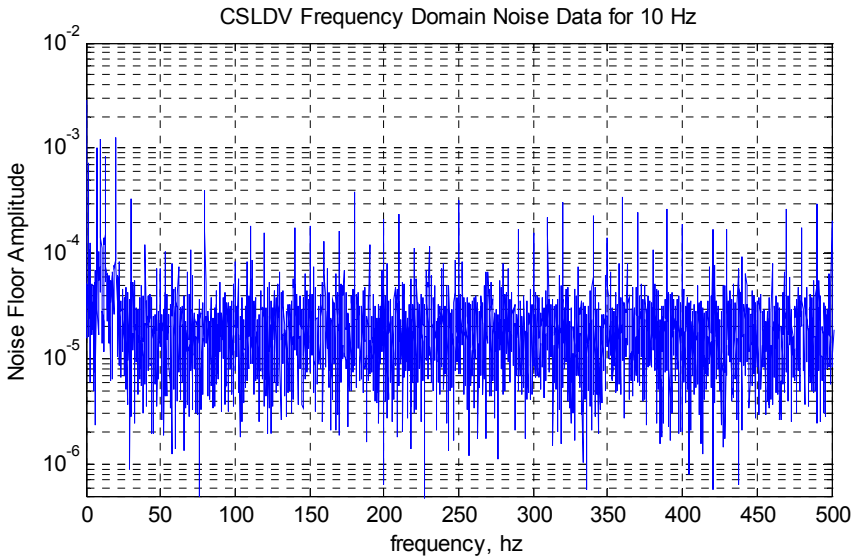

Figure 6: Vibrometer response for a 10 Hz sinusoidal CSLDV scan on a non-vibrating Aluminum beam. Peaks occur at the scan frequency and its harmonics and fill the entire bandwidth of the measurement.

Figure 7 shows the same response in the time domain, although with each period of the response plotted with a different color marker. Blue markers correspond to early times within the record, red ones with late times. A 10 Hz scan frequency was used, and the measurements were sampled at 12.8 kHz for a total sample time of 5.12 seconds to produce the plots in Figure 6 and 7, so 50 full periods of the scan were acquired, each period containing the forward and backward path with 1280 points per cycle. The lower-left portion of Figure 7 contains the corresponding mirror drive signal for the period of the scan, which is maximum when the laser spot is near the edges of the beam. The density plot reveals a noise signal that appears random besides a periodically varying envelope function. The envelope is maximum when the drive signal is zero, or when the mirror velocity is largest, and minimum when the mirror velocity is smallest. However, a closer inspection of the density plot (right pane, showing a small period of time near where the noise was maximum) reveals an underlying structure in the noise; there is significant scatter at each point, but the plot shows that the noise signal repeats itself to a significant extent each period. This structure explains the apparent periodicity of the noise, although the variance at each point along the beam is certainly significant. One should also note that the average spatial density in this resampled response is 200 micro-meters, so it is still three orders of magnitude larger than the laser wavelength.

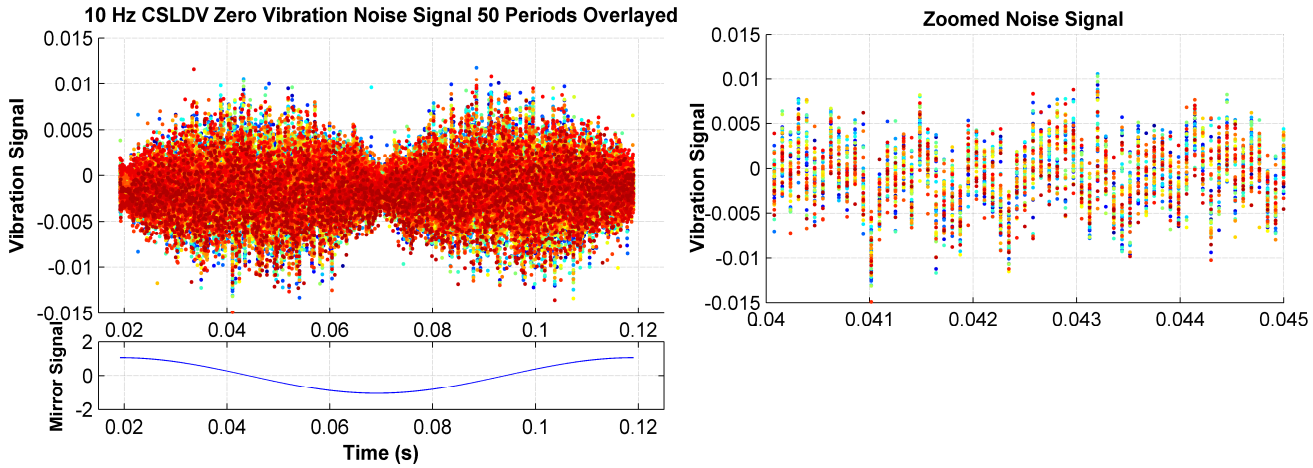

Figure 7: (left-top) Density plot of 101 periods of a 10 Hz sinusoidal noise scan overlaid. (left-bottom) Voltage input to scanning mirrors per period. (right) Zoomed region of the density plot.

3.1.1.1. Discussion

It appears that the amplitude envelope seen in Figure 7 is caused by variation in the surface velocity of the laser spot. To confirm this, a similar test was performed with a 10 Hz symmetric triangle function, which has a constant derivative (except for the discontinuity at the triangle peak). The frequency spectrum of this signal is provided in Figure 8.

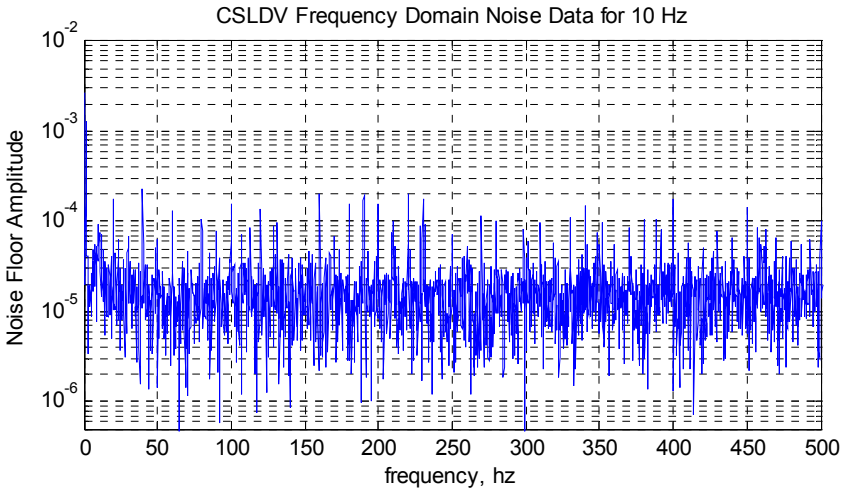

Figure 8: Frequency domain noise signal for a 10 Hz triangular input signal.

The frequency spectrum for the triangular scan also has the quasi-periodic form that is characteristic of laser speckle noise, containing notable peaks at the scan frequency and its harmonics, but the fundamental frequency and first few harmonics are not notably larger than the remaining harmonic peaks as they were for the sinusoidal scan in Figure 6. Also, the harmonic peaks do not protrude from the noise floor quite as much as those for the sinusoidal scan.

Figure 9 shows a time density plot of the noise signal obtained when the triangular mirror signal was used, the derivative is equal to a negative constant $-a$ for the first half of the period and a positive constant $+a$ for the second half of the signal. The noise signal is therefore modulated by a constant amplitude function, and does not show evidence of maximum or minimum levels. However, the detailed view shows that there is still considerable small-scale structure in the speckle noise, agreeing with other work [17] that also observed that the speckle noise signal was approximately periodic for a constant surface velocity of the laser spot.

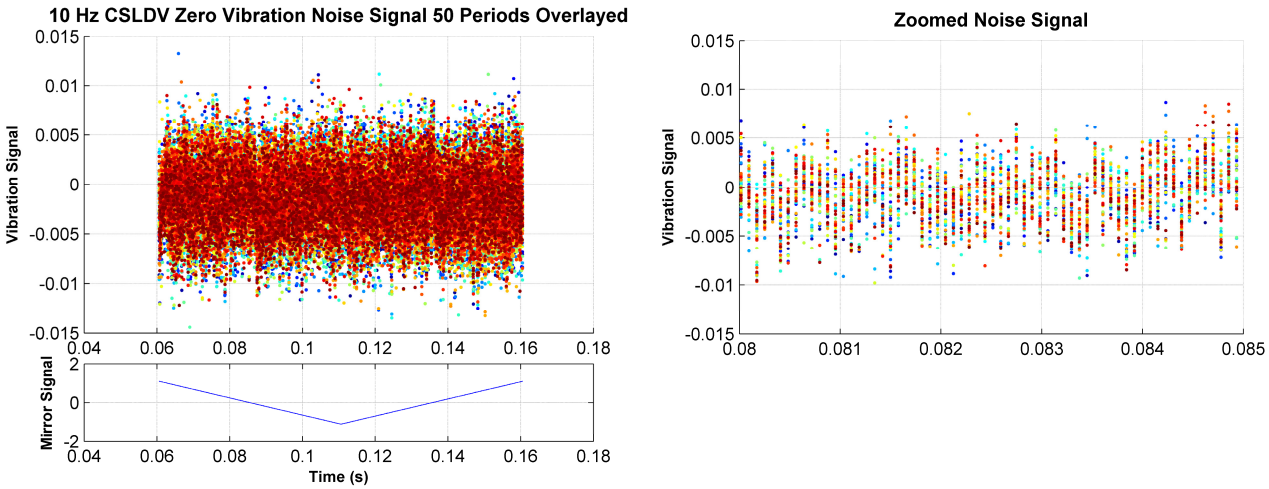

Figure 9: (left-top) Density plot for 50 periods of a 10 Hz triangular noise scan. (left-bottom) Voltage input to scanning mirrors per period. (right) Zoom on a region of the density plot.

As sensitive as speckle noise can be to small deviations from an exact periodic scan pattern, the frequency spectrums and time-domain responses shown here all contain a significant amount of periodicity. The noise amplitude, especially components near the fundamental scan frequency, is sensitive to the rate at which speckles transition through the detector and scan types should be chosen accordingly. Driving functions with time varying velocities seem to enhance the periodic component of noise, particularly at the fundamental scan frequency.

3.2. Experimental Setup/Geometry Noise Results

This section seeks to reveal the trends that occur when one of the test parameters effecting noise is varied while the others are held constant However, the variables that speckle noise depends on are not easily decoupled to illustrate individual influences, so it is difficult to quantify the effects of changing any individual parameter.

Quantitative measures of noise were calculated for both the periodic and non-periodic components. The non-periodic speckle noise component was calculated in the frequency domain for both the original and the lifted signals. The average amplitude of the non-periodic noise, η_{ave}, is calculated by removing both the harmonic peaks and their side bands from the frequency domain data series, leaving the non-periodic signal vector $Y_{aper}(\omega)$ at N_{aper} data points, and finding the arithmetic mean of the magnitude of the signal.

$$\eta_{ave} = \frac{\sum_{k=1}^{N_{aper}} \left| Y_{aper}(\omega_k) \right|}{N_{aper}} \tag{8}$$

The lifting process produces many pseudo-responses from a single noise signal, each of which aliases the noise into limited frequency band. Figure 1 showed the average magnitude, or composite of many of these pseudo-FRFs for a vibration signal. The periodic noise is aliased to the zero frequency line and falls off to the noise floor as in the red curve in Figure 1. Eq. (8) can be applied to the noise floor signal, $Y_{aper,lifted}(\omega)$ comprising $N_{aper,lifted}$ data points to give the lifted non-periodic noise, $\eta_{ave,lifted}$.

The periodic component of noise was quantified in the time domain by retaining those harmonic peaks that were removed from the signals to calculate the non-periodic noise and setting the remaining frequency lines to zero. This periodic signal was then transformed back into the time domain with the inverse Fast Fourier transform (IFFT). The standard deviation of the resulting signal was then found providing a metric of the periodic noise level, ρ_{ave}.

$$\rho_{ave} = \left(\frac{1}{N-1} \sum_{k=1}^{N} \left(y_{per}(t_k) - \bar{y}_{per} \right)^2 \right)^{\frac{1}{2}} \qquad (9)$$
$$y_{per}(t_k) = IFT\left(Y_{per}(\omega_k) \right)$$

3.2.1. Target-to-Detector Distance and Scan Length

3.2.1.1. Periodic Speckle Noise

Figure 10 provides the amplitude of the periodic noise using eq. (9) for the three scan lengths on the left and for only the scan length of 2*x_m=0.6 meters on the right, at each of the three target-to-detector distances. Martarelli and Ewins provided a similar data series in [18] for scanning frequencies of fscan=0.2, 0.5, 1, 5, 10, and 20 Hz. Note that 5, 10, 15, and 20 Hz corresponds to the first 4 points in the left plot of the blue curves. Note that the surface velocity depends on both the scan frequency and scan length, so each case gives a different maximum surface velocity for a given scan frequency. Also, the blue series for d=2 meters and 2*x_m=0.98 meters is truncated because the mirrors were not capable of scanning faster than 60 Hz at that wide of an angle.

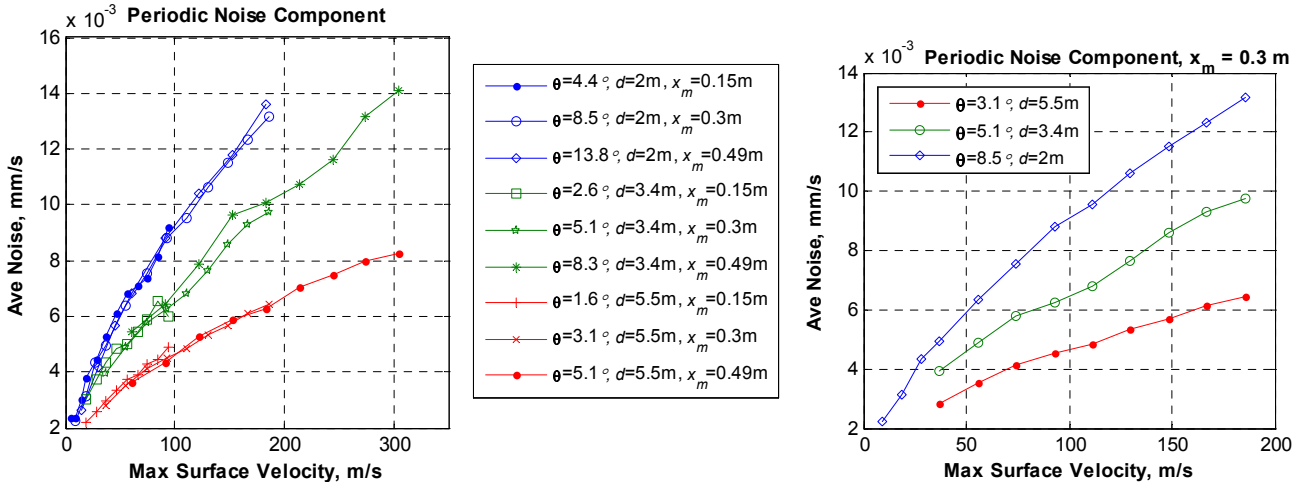

Figure 10: (*left*) Periodic time domain noise components for three target-to-detector separations and three scan lengths. (*right*) Data re-plotted for only one scan length.

The left plot in Figure 10 shows that the curves for a given target-to-detector distance cluster together, independent of the scan length, so the noise seems to be only a function of the surface velocity and the target-to-detector separation. For any given data series the periodic component of noise increases rather sharply with increasing surface velocity, similar to what was observed in [18]. The right portion of the figure illustrates three scans in which only the target-to-detector distance was varied; the scan length was held constant at 2*x_m=0.6 meters. Clearly, the noise trend decreases when the target-to-detector distance is increased for a given surface velocity. This reveals that one can obtain lower noise levels at a given maximum surface velocity simply by increasing the separation between the laser and the test article.

3.2.1.2. Non-Periodic Speckle Noise – Frequency Domain

The non-periodic speckle noise as calculated by eq. (8) is plotted in Figure 11. The plot contains data series for the three scan lengths at the target-to-detector distance d=2 meters and the short scan length 2*x_m= 0.3 meters for the remaining two target-to-detector distances. Again, the noise level generally increases with increasing surface velocity. For a fixed scan length (2*x_m= 0.3 meters in the plot), the noise level is larger for smaller target-to-detector distances, as was also the case for the periodic component of the noise. For a fixed target-to-detector distance (data in blue),longer scan lengths corresponded to increased noise, and this trend seems even more significant than the dependence on target-to-detector separation. This behavior is qualitatively very different than that which was observed for the periodic component of the speckle noise. The lowest velocity point in the curve for 2*x_m= 0.3 meters and d=2 meters appears to be an outliner, the cause for which is not known.

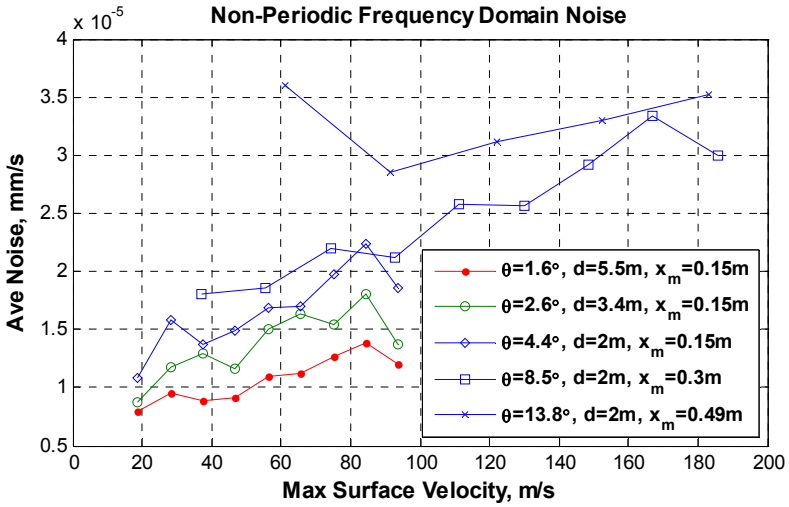

Figure 11: Non-Periodic frequency domain noise components.

3.2.1.3. Non-Periodic Noise – Lifted Frequency Domain

The non-periodic lifted noise was calculated by applying eq. (8) to the composite of the pseudo-FRFs, and is shown in Figure 12. These are the same signals shown in Figure 11, but this shows the noise level in the lifted signals whereas Figure 11 showed the noise level in the original signal. The effect of noise on the lifted signal is more important when using the method in [7, 8] to extract the modes, because any modes that fall below the noise floor are not observed. Again, for a fixed scan length of $2*x_m$= 0.3 meters, the noise level increases for smaller target to detector distances. For a fixed target-to-detector distance, the noise amplitude increases for increasing scan length, and this effect is once again more significant than the dependence on target-to-detector separation. Furthermore, besides the outlier at $2*x_m$= 0.98 meters and d=2 meters, the noise level does not change appreciably with surface velocity; quite a different behavior than that which was noted above for both the periodic and non-periodic noise.

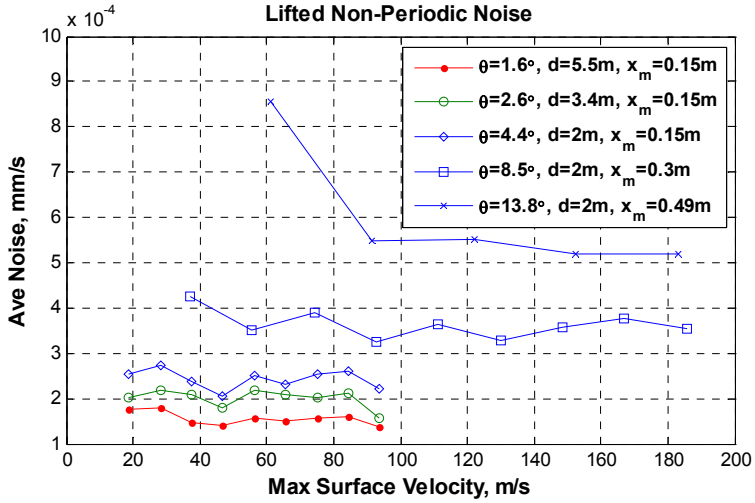

Figure 12: Non-Periodic lifted frequency domain noise component for three scan lengths at each of three target-to-detector separations.

3.2.1.4. Discussion

For a given set of experimental parameters, that is for any target-to-detector separation d, scan length $2*x_m$, and for a single surface, both the periodic and non-periodic noise tend to increase with maximum surface velocity in the frequency domain as seen in Figures 10 and 11. This agrees with prior research by Martarelli and Ewins [18].

However, Figure 12 suggests that the non-periodic noise in the lifted signals does not vary significantly as the maximum surface velocity is increased, suggesting that it matters little what surface velocity (scan frequency) one uses when the lifting method is used to extract the modes. The reason for this is not yet understood, but one can gain some insight by observing the noise in the lifted signals in the time domain in Figures 7 and 9 . The spread in each column of points is an indicator of the noise level in one lifted response. The results in Figure 12 suggest that the variance revealed by the height of each column of points should not change with scan frequency, even though the overall pattern of the noise signal may change. This should be explored further in subsequent works.

It is important to note that one must remove sidebands from the scan frequency harmonics to properly compute the non-periodic portion of the noise. The non-periodic noise was found to increase less dramatically with the maximum surface velocity than the periodic noise and seems to depend more heavily on the scan length than it does on target-to-detector separation. This may be explained, in part, by the fact that increased scan lengths require increased sweep angles if the target-to-detector separation is held constant, causing the laser spot to come out of focus at the edges of the beam resulting in a speckle pattern such as that shown in Figure 5. When seeking to maximize the scan frequency, as is desirable for the lifting method, these results show that it is advantageous to keep line scans as short as possible and to position the LDV as far as possible from the test device. More importantly, these results illustrate how much of an increase in noise to expect as these parameters are varied.

3.3. Experimental Sampling Frequency Noise Results

As discussed previously, the spatial resolution of a CSLDV measurement is limited only by the bandwidth of the LDV and the scan frequency, suggesting that one could obtain any desired level of resolution by increasing the sampling rate of the LDV. This was investigated by observing the noise level at sampling frequencies of 12.8, 25.6, and 51.2 kHz for a fixed target-to-detector distance of d=2 meters and scan length of 2*x_m= 0.3 meters. The noise was recorded for all of the scanning frequencies in Table 2 for each sampling frequency. The top pane in Figure 13 shows the FFT of the noise signals for a 100 Hz scan frequency at the different sample rates. Both the “pseudo-vibration” peaks occurring at the harmonics of the 100 Hz scanning frequency, and the noise at in between these peaks extend for the full sampling bandwidth without decreasing in amplitude. The lower cluster of plots display the noise signal in the time domain, similar to that of Figures 7 and 9. The mirror angle achieves a maximum value at about 1.2 milliseconds, where the first minimum of the noise envelope resides. The envelope on the noise amplitude is present for all three sampling rates but becomes more prominent as the sampling frequency is increased. There are also a few periodic features in the noise profile that are visible at all three sample rates, such as the peak at 8.6 ms.

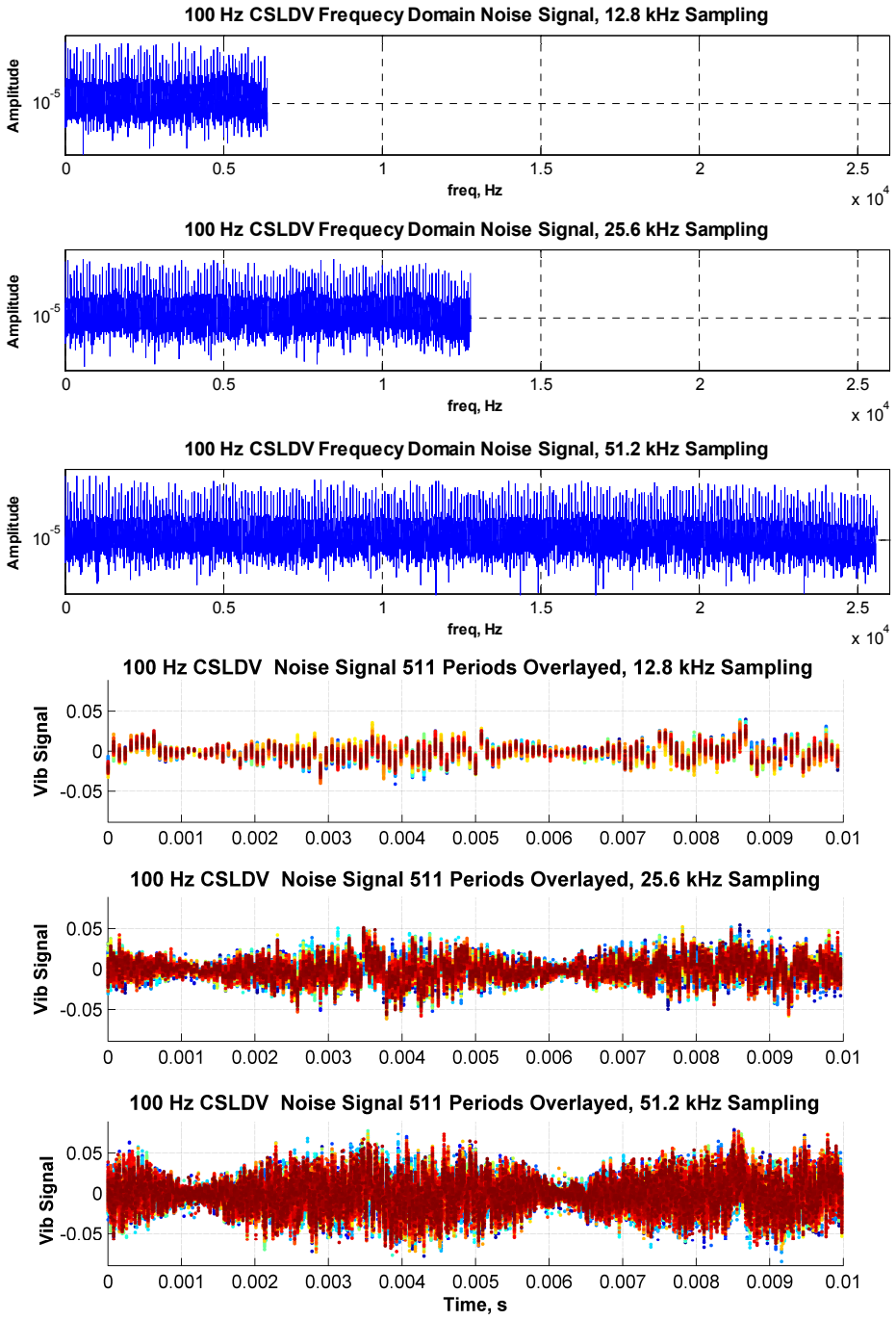

Figure 13: Sampling frequency effects on 100 Hz CSLDV noise signals. (*top)* Frequency domain spectrums. (*bottom*) Periodic density plots with 511 periods superposed.

Using the same procedures as in Section 3.2, the periodic and lifted non-periodic noise components were calculated for each test. Figure 14 provides the results of the noise calculations for the three sampling frequencies. The left plot contains the periodic noise component calculated with eq. (9), revealing that the periodic noise increases with the maximum surface velocity. The noise level is always higher when sampled at higher frequencies. The right plot, which provides the lifted non-periodic noise, also shows the noise increasing with sampling frequency, but the lifted noise does not increase with surface velocity. The noise data sampled at 51.2 kHz seems to decrease in magnitude with increasing surface velocity.

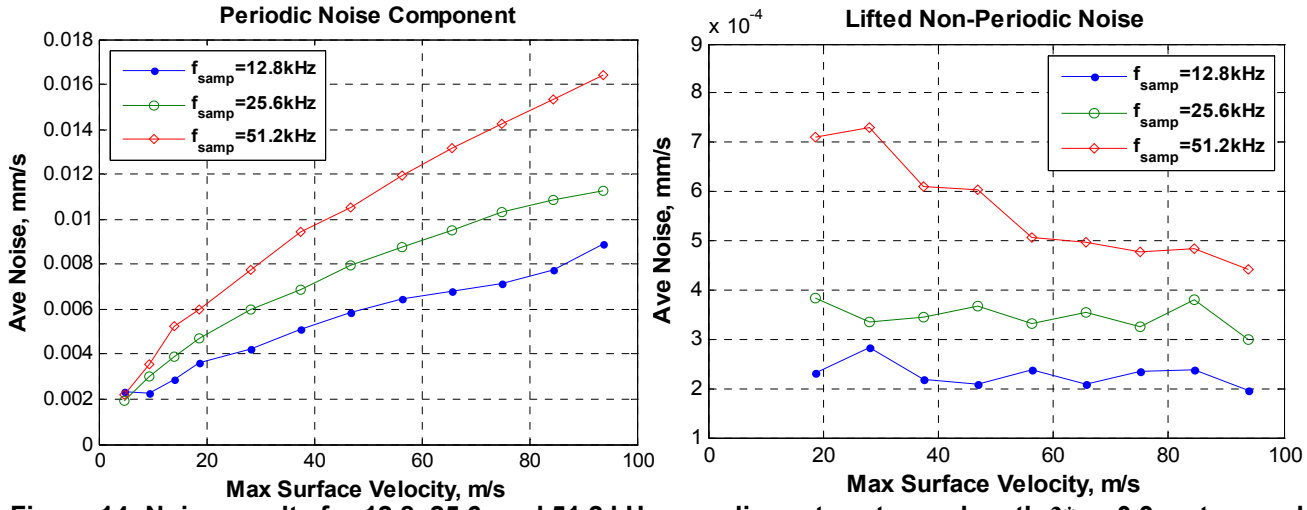

Figure 14: Noise results for 12.8, 25.6, and 51.2 kHz sampling rates at scan length $2*x_m$=0.3 meters and target to-detector-distance d=2 meters. (*left*) Periodic time domain noise component. (*right*) Lifted non-periodic frequency domain noise.

3.3.1. Discussion

These results reveal that the laser speckle noise has seemingly infinite extent in the frequency domain. As the sample rate increases, one seems to capture the speckle noise more fully, so the noise level seems to increase. However, this noise affects the experiment differently depending on how the mode shapes are extracted. Figure 13 shows that the amplitude of the harmonic and off-harmonic noise is basically constant with frequency, so if the method of Stanbridge et al. [5, 6] is employed, then it would seem that increasing the bandwidth beyond some minimum value would simply add frequency lines with no meaningful information, because any vibration information carried at the added frequencies is masked by the noise. When the lifting approach is used, one might expect to be able to increase the spatial resolution by increasing the sampling rate, For example, a 100 Hz continuous scanning signal sampled at 25.6 kHz will result in N_o = 256 pseudo-response points per scan cycle, while the same signal sampled at 51.2 kHz produces N_o = 512 pseudo-response points. However, Figure 14 show that the noise level increases substantially with increasing sampling rate. To determine the optimum sample rate, one must consider that increasing the bandwidth doubles the point resolution, so two points are now available to estimate the mode shape at each point in a measurement at a lower sample rate, and the redundant points could be averaged decreasing the variance by a factor of $1/2^{1/2}$ = 0.707 or about 30%. However, Figure 13 reveals that doubling the sample rate increases the non-periodic noise by about 75%, so the best results are probably obtained if the sampling rate is the minimum that captures the important Fourier terms describing each mode (see eq. (4)).

The non-periodic lifted noise component increases with the sampling frequency. The same data series are plotted in the left and right portions of Figure 14, but the first three data points are omitted in the lifted frequency domain because the side bands of the scan frequency harmonics filled the entire (aliased) spectrum of the lifted signal. For example, a test with a scan frequency of 5 Hz has a lifted bandwidth of 2.5 Hz and side bands of "pseudo-vibrations" have been observed to surround a given harmonic by (+/-) 2 Hz or more.) When this is the case, the noise floor cannot accurately be determined and so it was not shown.

4. Conclusion

Speckle noise is a very complex phenomenon that affects CSLDV measurements. This work has revealed that speckle noise in CSLDV applications is dependent on the laser spot surface velocity (or rate of speckle transition through the detector), the distance from the target device to the detector, the length of the scan on the target device, and the sampling rate of the data acquisition system. Previous works by Rothberg and his associates suggested that speckle noise may be reduced by changing the laser spot size for certain types of speckle evolution, but no significant dependence on the laser spot size was observed here.

The speckle noise in a CSLDV measurement has both periodic and non-periodic components. The periodic component of the noise represents the speckle patterns seen by the laser at it presumably scans the exact same path each cycle. The magnitude of the periodic noise increases severely with surface velocity, in agreement with what was observed by Ewins and Martarelli, but can be decreased by increasing target-to-detector distance. The non-periodic noise seems to be caused by other factors, perhaps by stray from a truly periodic speckle pattern due to small inconsistencies in the laser's scan path. This noise was found to increase only modestly with surface velocity and more significantly with increased scan lengths, and decreased as the target-to-detector separation was increased. However, when the CSLDV measurements are decomposed using the lifting method, the noise appears to be constant with scan frequency, advocating the use of the highest scan frequency possible. However, increasing the sampling rate increased the noise level in the lifted signals, so one should use care to not sample faster than necessary to capture the meaningful vibration signal.

The reasons for many of the trends observed here are not at all clear, and sometimes even seem counter-intuitive. The decrease in noise with increased separation of the test device and the LDV may be due to reduced Doppler signal amplitude or possibly to a change in the character of the speckle motions (e.g. from boiling motions to translating speckles). Increasing the scan length could serve to increase the number of speckle patterns observed in a given time interval, so it does seem reasonable that this would increase the speckle noise. However, the periodic component of the speckle noise was found to be largely insensitive to the scan length. The laser spot size and focal point was confirmed to have a significant effect on the size and nature of the speckle pattern observed at the detector, yet this did not affect the speckle noise noticeably in any of the tests performed here. It is also quite surprising that the demodulator employed in the LDV seems to keep the speckle noise contained to the scan harmonics, so that the noise at other frequencies remains essentially constant with increasing surface velocity even though the harmonic noise is increasing sharply. Fortunately, even though all of these factors are not understood completely, one can make use of the trends illustrated in this work to design successful CSLDV tests in many circumstances.

References

[1] A. B. Stanbridge, M. Martarelli, and D. J. Ewins, "Measuring area vibration mode shapes with a continuous-scan LDV," *Measurement,* vol. 35, pp. 181-9, 2004.

[2] P. Sriram, J. I. Craig, and S. Hanagud, "Scanning laser Doppler vibrometer for modal testing," *International Journal of Analytical and Experimental Modal Analysis,* vol. 5, pp. 155-167, 1990.

[3] P. Sriram, S. Hanagud, and J. I. Craig, "Mode shape measurement using a scanning laser Doppler vibrometer," *Proceedings of the 9th International Modal Analysis Conference,* Florence, Italy, 1991, pp. 176-181.

[4] P. Sriram, S. Hanagud, and J. I. Craig, "Mode shape measurement using a scanning laser Doppler vibrometer," *International Journal of Analytical and Experimental Modal Analysis,* vol. 7, pp. 169-178, 1992.

[5] R. Ribichini, D. Di Maio, A. B. Stanbridge, and D. J. Ewins, "Impact Testing With a Continuously-Scanning LDV," in *26th International Modal Analysis Conference (IMAC XXVI)* Orlando, Florida, 2008.

[6] A. B. Stanbridge, M. Martarelli, and D. J. Ewins, "Scanning laser Doppler vibrometer applied to impact modal testing," in *17th International Modal Analysis Conference - IMAC XVII*. vol. 1 Kissimmee, FL, USA: SEM, Bethel, CT, USA, 1999, pp. 986-991.

[7] M. a. S. Allen, Michael, "Mass normalized mode shapes using impact excitation and continuous-scan laser Doppler vibrometry," in *Italian Association of Laser Velocimetry and non-Invasive Diagnostics (AIVELA)* Ancona, Italy, 2008.

[8] M. S. Allen and M. W. Sracic, "A Method for Generating Pseudo Single-Point FRFs from Continuous Scan Laser Vibrometer Measurements," in *26th International Modal Analysis Conference (IMAC XXVI)*, Orlando, Florida, 2008.

[9] M. S. Allen, "Floquet Experimental Modal Analysis for System Identification of Linear Time-Periodic Systems," in *ASME 2007 International Design Engineering Technical Conference*, Las Vegas, NV, 2007.

[10] M. S. Allen and J. H. Ginsberg, "A Global, Single-Input-Multi-Output (SIMO) Implementation of The Algorithm of Mode Isolation and Applications to Analytical and Experimental Data," *Mechanical Systems and Signal Processing,* vol. 20, pp. 1090–1111, 2006.

[11] L. A. Luxemburg, "Frequency Analysis of Time-Varying Periodic Linear Systems by Using Modulo p Transforms and Its Applications to the Computer-Aided Analysis of Switched Networks," *Circuits, Systems, and Signal Processesing,* vol. 9, pp. 3-29, 1990.

[12] P. a. T. Arambel, G., "Robust H_{oo} Identification of Linear Periodic Discrete-Time Systems," *International Journal of Robust and Nonlinear Controol,* vol. 4, pp. 595-612, 1994.
[13] P. a. R. Martin, S., "Laser Vibrometry: speckle noise maps for in-plane and tilt target motions," in *OPTIMESS,* Leuven, Belgium, 2007.
[14] P. a. R. Martin, S., "Laser Vibrometry and the secret life of speckle patterns," in *Eigth International Conference on Vibration Measurements by Laser Techniques: Advances and Applications* Ancona, Italy, 2008.
[15] S. J. Rothberg and B. J. Halkon, "Laser vibrometry meets laser speckle," *Sixth International Conference on Vibration Measurements by Laser Techniques: Advances and Applications*, Ancona, Italy, 2004, pp. 280-91.
[16] N. Takai, Iwai, T., and Asakura, T., "Correlation distance of dynamic speckles," *Applied Optics,* vol. 22, pp. 170-177, 1983.
[17] S. J. Rothberg, "Laser vibrometry. Pseudo-vibrations," *Journal of Sound and Vibration,* vol. 135, pp. 516-522, 1989.
[18] M. Martarelli and D. J. Ewins, "Continuous scanning laser Doppler vibrometry and speckle noise occurrence," *Mechanical Systems and Signal Processing,* vol. 20, pp. 2277-89, 2006.
[19] M. Allen and J. H. Ginsberg, "Floquet Modal Analysis to Detect Cracks in a Rotating Shaft on Anisotropic Supports," in *24th International Modal Analysis Conference (IMAC XXIV)*, St. Louis, MO, 2006.
[20] R. Guenther, *Modern Optics* vol. 1. New York: John Wiley & Sons, Inc., 1990.